

Cover
The structures of squalene and hopene against a background of hops.

Free site-wide access to Advance Articles and the electronic form of this journal is provided with a full-rate institutional subscription.
See www.rsc.org/ejs for more information

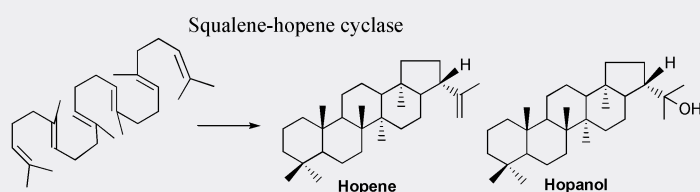
contents

FEATURE ARTICLE

291

Squalene–hopene cyclase: catalytic mechanism and substrate recognition

Tutomu Hoshino and Tutomu Sato



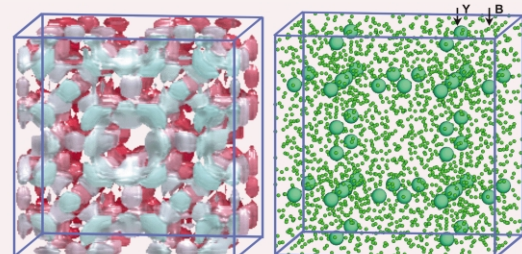
Rapid progress on the catalytic mechanism and substrate recognition by squalene–hopene cyclase, which has occurred only in the last several years, is reported. A series of site-directed mutation experiments and some squalene analogues have provided deep insight into the polycyclization mechanism and catalytic sites in conjunction with the information from X-ray crystal data.

COMMUNICATIONS

302

Three-dimensional imaging of YB₅₆ by high-resolution electron microscopy

Takeo Oku

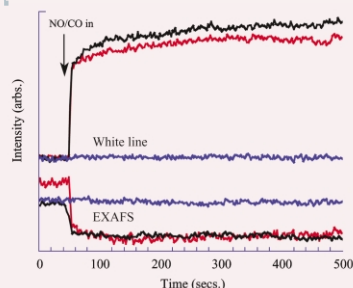


The three-dimensional potential map of a YB₅₆ crystal with a size below 20 nm was obtained by inverse Fourier transformation of three-dimensional phases and amplitudes, this method is useful for three-dimensional structural analysis of nanocrystals.

304

Susceptibility of a heterogeneous catalyst, Rh/γ-alumina, to rapid structural change by exposure to NO

Tom Campbell, Andrew J. Dent, Sofia Diaz-Moreno, John Evans, Steven G. Fiddy, Mark A. Newton and Sandra Turin



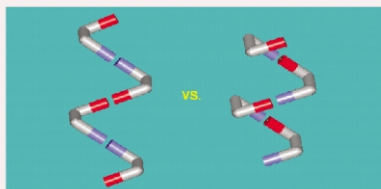
Metal particles in a Rh/γ-Al₂O₃ catalyst of differing particle size are oxidised by NO/He within 5 seconds at 313 K; rapid, highly exothermic dissociative chemisorption of NO is the initial step.

306



Helix versus zig-zag: control of supramolecular topology via carboxylic acid conformations in *ortho*-substituted phenyl amines

Jason E. Field and D. Venkataraman

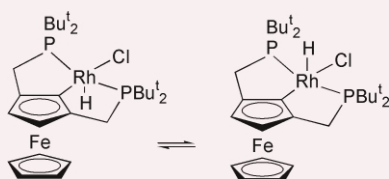


Depending on the conformation of the carboxylic acids, bridged bis(benzoic acid) systems can potentially form three types of supramolecular motifs, including the helix. Through internal hydrogen bonding, this conformation, and thus the overall supramolecular structure, may be controlled.

308

Synthesis and reactivity of a ferrocene-derived PCP-pincer ligand

Edward J. Farrington, Eloisa Martinez Viviente, B. Scott Williams, Gerard van Koten and John M. Brown

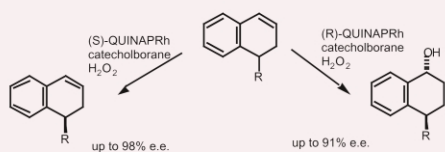


A ferrocene analogue of well-established pincer ligands shows two equilibrating diastereomers in its chlororhodium complex.

310

Efficient kinetic resolution in hydroboration of 1,2-dihydronaphthalenes

Kenji Maeda and John M. Brown



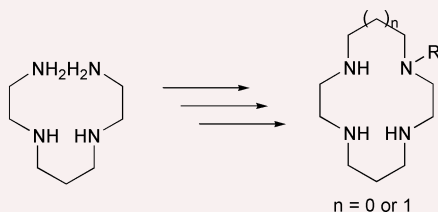
1-Substituted 1,2-dihydronaphthalenes undergo kinetic resolution during asymmetric hydroboration with Rh-QUINAP complexes.

312



An organic template approach for the synthesis of selectively functionalised tetraazacycloalkanes

Frédéric Boschetti, Franck Denat, Enrique Espinosa and Roger Guilard

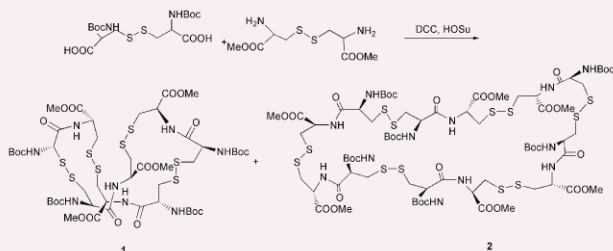


Selectively functionalised tetraazacycloalkanes are obtained from the open-chain tetraamine by using a bisaminal moiety acting both as a template agent and as a N-protecting group.

314

Unusual cyclo-tetra and hexa peptidation of bis-boc-cystine with cystine-di-OMe: one step preparation of the novel 32- and 48-membered cyclotetracystine and cyclohexacystine

S. Ranganathan, K. M. Muraleedharan, M. Vairamani, A. C. Kunwar and A. Ravi Sankar

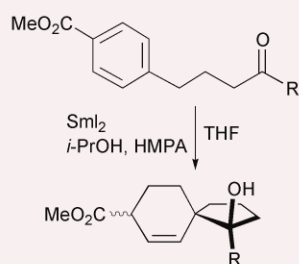


The unprecedented formation of 32- and 48-membered macrocycles that inscribe 4 and 6 cystine units, in the peptidation of bis-Boc-cystine with cystine-di-OMe is reported.

316

The first samarium(II)-mediated stereoselective spirocyclization onto an aromatic ring

Hiroaki Ohno, Shin-ichiro Maeda, Mitsuaki Okumura, Ryutaro Wakayama and Tetsuaki Tanaka

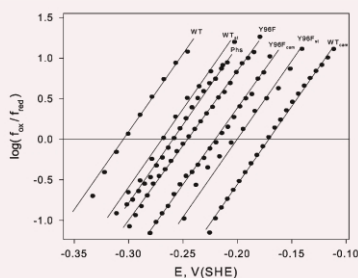


The first samarium(II)-mediated spirocyclisation onto an aromatic ring was achieved by the reaction of methyl 4-(4-oxoalkyl)benzoates with SmI_2 in the presence of *i*-PrOH and HMPA.

318

Redox control of the P450cam catalytic cycle: effects of Y96F active site mutation and binding of a non-natural substrate

Vytautas Reipa, Martin P. Mayhew, Marcia J. Holden and Vincent L. Vilker

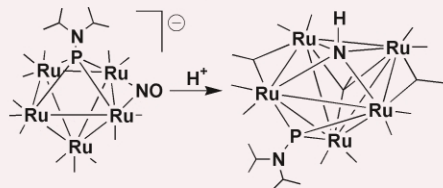


Nernst plots of purified cytochrome P450cam and Y96F mutant with and without camphor or styrene as substrates.

320

Mixed nitrosyl/phosphinidene and nitrene/phosphinidene clusters of ruthenium

Ludmila Scoles, Brian T. Sterenberg, Konstantin A. Udachin and Arthur J. Carty

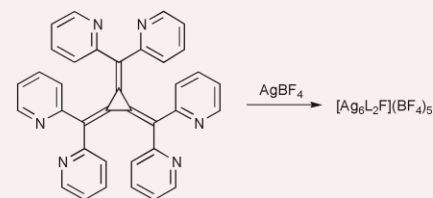


Reaction of $[\text{Ru}_5(\text{CO})_{15}(\mu_4\text{-PNPr}^t_2)]$ with $[\text{PPN}][\text{NO}_2]$ led to the cluster complex $[\text{PPN}][\text{Ru}_5(\text{CO})_{13}(\mu\text{-NO})(\mu_4\text{-PNPr}^t_2)]$ which is transformed into the novel cluster $[\text{Ru}_5(\text{CO})_{10}(\mu\text{-CO})_2(\mu_3\text{-CO})(\mu_4\text{-NH})(\mu_3\text{-PNPr}^t_2)]$ via treatment with triflic acid.

322

Hexa(2-pyridyl)[3]radialene: self-assembly of a hexanuclear silver array

Peter J. Steel and Christopher J. Sumbly

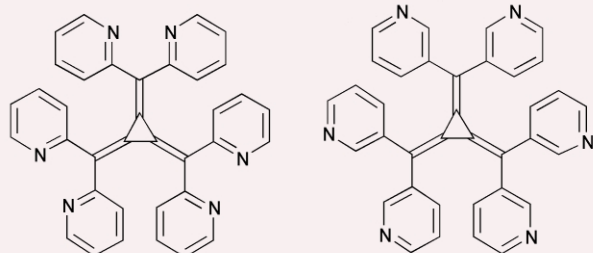


Reaction of the new ligand hexa(2-pyridyl)[3]radialene with silver tetrafluoroborate results in the formation of a M_6L_2 cage with an encapsulated μ_3 -fluorido anion.

324

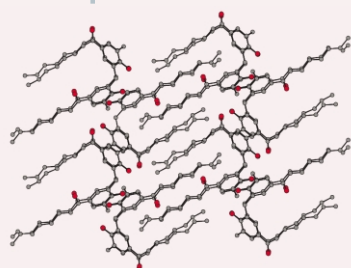
Hexakis(2-pyridyl)- and hexakis(3-pyridyl)[3]radialene: novel, water-soluble [3]radialenes with potential utility for supramolecular chemistry

Kouzou Matsumoto, Yukako Harada, Takeshi Kawase and Masaji Oda



These radialenes, the first members of radialenes having azine groups, are stable, moderately electron poor radialenes showing the corresponding anion radicals and dianions upon both electrochemical and alkali metal reduction.

326

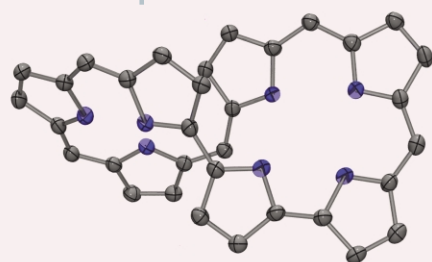


Para-acyl calix[4]arenes: amphiphilic self-assembly from the molecular to the mesoscopic level

Patrick Shahgaldian, Michele Cesario, Philippe Goreloff and Anthony W. Coleman

Non-contact mode imaging of amphiphilic solid nanoparticles shows flattened spherical structures of 190 nm in diameter and 50 nm in width, the crystal structure of the molecules shows an unusual partially interdigitated tilted packing system.

328

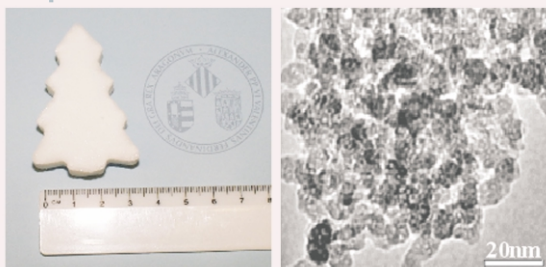


[30]Heptapyrin(1.1.1.1.0.0): an aromatic expanded porphyrin with a 'figure eight' like structure

Christophe Bucher, Daniel Seidel, Vincent Lynch and Jonathan L. Sessler

The new heptapyrrolic macrocycle, [30]heptapyrin(1.1.1.1.0.0), is aromatic as judged from its spectral features. Nonetheless, it adopts a 'figure eight'-like structure in the solid state.

330

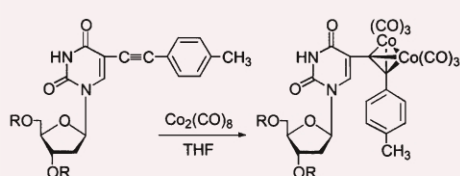


Silica-based powders and monoliths with bimodal pore systems

Jamal El Haskouri, David Ortiz de Zárate, Carmen Guillem, Julio Latorre, Maite Caldés, Aurelio Beltrán, Daniel Beltrán, Ana B. Descalzo, Gertrudis Rodríguez-López, Ramón Martínez-Mañez, M. Dolores Marcos and Pedro Amorós

A simple chemical technique for obtaining new bimodal porous silica-based materials admitting variable contents of different heteroelements is presented. The resulting materials can be easily moulded as porous monoliths of significantly large dimensions.

332

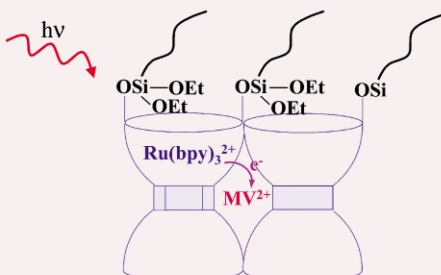


Synthesis of dicobalt hexacarbonyl 5-*p*-tolylethynyl-2'-deoxyuridine

Noor Esho, Brian Davies, Janet Lee and Roman Dembinski

Reactions of 5-*p*-tolylethynyl-2'-deoxyuridine and 3',5'-di-*O*-acetyl-5-*p*-tolylethynyl-2'-deoxyuridine with $\text{Co}_2(\text{CO})_8$ in THF gave 5-*p*-tolC₂[Co₂(CO)₆]-2'-deoxyuridine and 3',5'-di-*O*-acetyl-5-*p*-tolC₂[Co₂(CO)₆]-2'-deoxyuridine (92 and 66%).

334



Evidence for through-framework electron transfer in intrazeolite photochemistry. Case of Ru(bpy)₃²⁺ and methylviologen in novel delaminated ITQ-2 zeolite

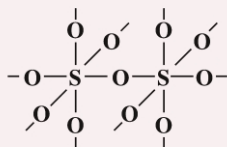
Avelino Corma, Vicente Fornés, María S. Galletero, Hermenegildo García and J. C. Scaiano

Emission and laser flash photolysis firmly proves that in zeolite, photoinduced electron transfer between a donor and an acceptor separated in non-connected compartments can occur through the walls.

336

Possible high-pressure structures of sulfur trioxide

Toomas Tamm and Pekka Pyykkö

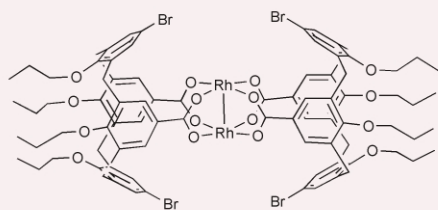


Calculations with the linearized augmented plane wave method indicate that several high-density forms of sulfur trioxide should be accessible at pressures above 29 GPa, with densities up to 1.7 times larger than the presently known forms of solid SO₃.

338

Calixarenes as ligands for transition-metal catalysts: a bis(calix[4]arene-11,23-dicarboxylato) dirhodium complex

Jürgen Seitz and Gerhard Maas

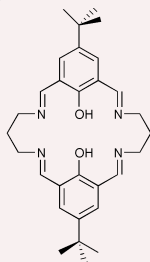


A novel dirhodium tetracarboxylate complex is described in which two calix[4]arene macrocycles are connected through upper-rim bridging by a Rh–Rh unit. It is potentially useful for diastereoselective and regioselective carbene transfer reactions with diazo compounds.

340

Compartmental Schiff-base ligands as selective double-loaded extractants for copper(II)

Daniel Black, Alexander J. Blake, Rachel L. Finn, Leonard F. Lindoy, Azizollah Nezhadali, Gholamhossein Rounaghi, Peter A. Tasker and Martin Schröder

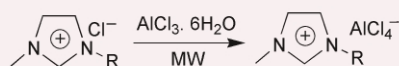


The Robson compartmental macrocyclic ligand derived from the condensation of derivatives of 2,6-diformylphenol and diamines has been prepared for the first time in its free ligand form, and shows efficient transport and extraction of Cu(II).

342

Microwave-assisted preparation of dialkylimidazolium tetrachloroaluminates and their use as catalysts in the solvent-free tetrahydropyranylation of alcohols and phenols

Vasudevan V. Nambodiri and Rajender S. Varma

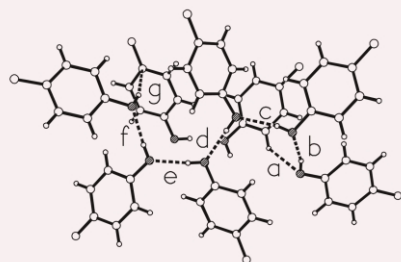


Microwave-assisted preparation of dialkylimidazolium tetrachloroaluminates and their use as catalysts in the solvent-free tetrahydropyranylation of alcohols and phenols is described.

344

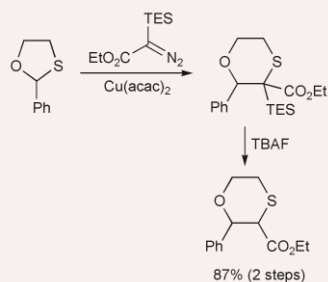
Unusually long cooperative chain of seven hydrogen bonds. An alternative packing type for symmetrical phenols

Praveen K. Thallapally, Amy K. Katz, H. L. Carrell and Gautam R. Desiraju



Conformational flexibility in a symmetrical tris-phenol leads to close packed structures that are also characterised by an extended though finite cooperative chain of hydrogen bonds.

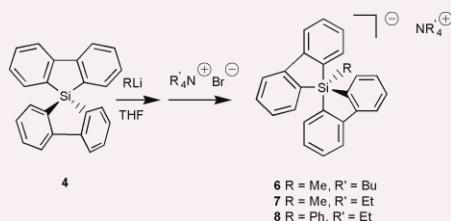
346

**A ring expansion reaction of 1,3-oxathiolanes**

Maria Ioannou, Michael J. Porter and Fabienne Saez

The carbene-mediated ring expansion of 1,3-oxathiolanes proceeds efficiently provided a silylated diazo compound is used. Subsequent removal of the silyl group can be achieved in high yield by fluoride treatment.

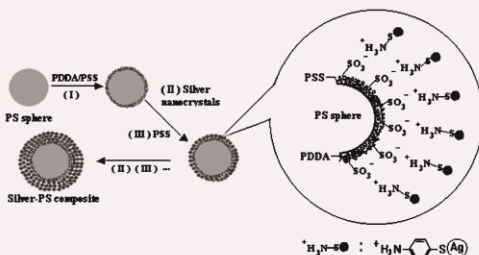
348

**Tetraalkylammonium pentaorganosilicates: the first highly stable silicates with five hydrocarbon ligands**

Sirik Deerenberg, Marius Schakel, Adrianus H. J. F. de Keijzer, Mirko Kranenburg, Martin Lutz, Anthony L. Spek and Koop Lammertsma

Several tetraalkylammonium pentaorganosilicates, derived from 9,9-spiro(9H,9-silafluorene) were prepared from the corresponding lithium silicates and isolated and characterized as storable high melting solids.

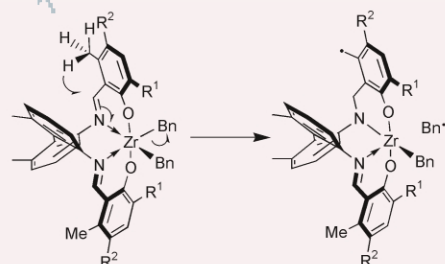
350

**Fabrication of compact silver nanoshells on polystyrene spheres through electrostatic attraction**

A. G. Dong, Y. J. Wang, Y. Tang, N. Ren, W. L. Yang and Z. Gao

Nanoshells composed of close-packed silver nanocrystals have been fabricated on PS spheres *via* direct electrostatic adsorption at appropriate pH; the thickness and roughness of the shell can be readily controlled through a layer-by-layer technique.

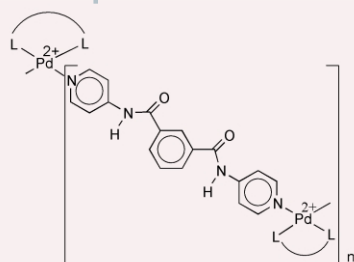
352

**Problems and solutions for alkene polymerisation catalysts incorporating Schiff-bases; migratory insertion and radical mechanisms of catalyst deactivation**

Paul D. Knight, Adam J. Clarke, Brian S. Kimberley, Richard A. Jackson and Peter Scott

Steric blocking of an intramolecular 1,2-migratory insertion reaction of a zirconium salicylaldiminato complex leads to a long-lived catalyst for ethene polymerisation, but promotes a new radical catalyst decomposition mechanism in certain instances.

354

**Crosslinking a palladium(II) polymer gives a laminated sheet structure**

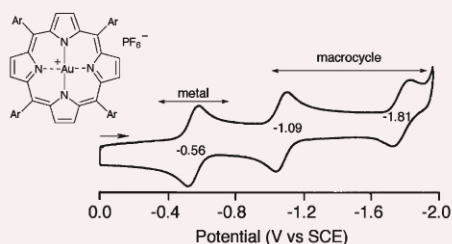
Zengquan Qin, Michael C. Jennings and Richard J. Puddephatt

Chains of a zigzag coordination polymer containing bis(pyridyl) bridging groups between palladium(II) centres can be arranged to give a laminated sheet structure by a biomimetic approach in which hydrogen bonding involving amide groups is the key feature.

356

Evidence that gold(III) porphyrins are *not* electrochemically inert: facile generation of gold(II) 5,10,15,20-tetrakis(3,5-di-*tert*-butylphenyl)porphyrin

Karl M. Kadish, Wenbo E, Zhongping Ou, Jianguo Shao, Paul J. Santic, Kei Ohkubo, Shunichi Fukuzumi and Maxwell J. Crossley

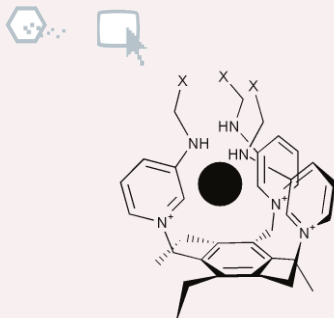


Reduction of a gold(III) porphyrin occurs at the central metal ion to give the first known gold(II) porphyrin overturning the long held assumption that reduction of such complexes only occurs at the macrocycle.

358

Anion sensing 'venus flytrap' hosts: a modular approach

Lagili O. Abouderbala, Warwick J. Belcher, Martyn G. Boutelle, Peter J. Cragg, Jaspreet Dhaliwal, Muriel Fabre, Jonathan W. Steed, David R. Turner and Karl J. Wallace

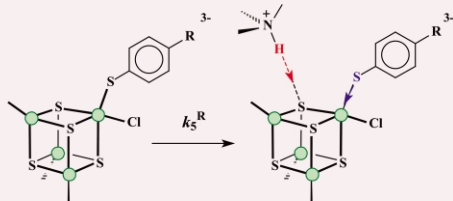


A series of readily assembled tripodal hosts for anions have been prepared. The new materials show a remarkable anion chelate effect.

360

Ligand movement modulates the rate of proton transfer in reactions of $[\text{Fe}_4\text{S}_4\text{Cl}_4]^{2-}$

Adrian J. Dunford and Richard A. Henderson

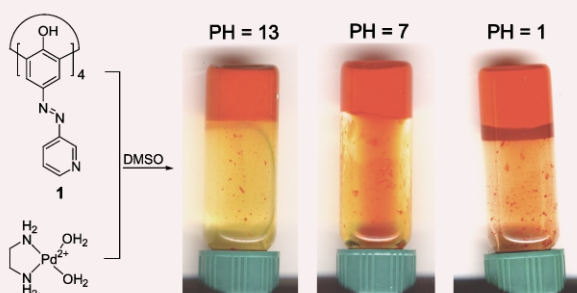


Both nucleophilic attack of $4\text{-RC}_6\text{H}_4\text{S}^-$ at $[\text{Fe}_4\text{S}_4\text{Cl}_4]^{2-}$ and subsequent protonation are facilitated by electron-withdrawing R-substituents, indicating that Fe-thiolate bond length changes modulate the rate of proton transfer.

362

A stable metal coordination polymer gel based on a calix[4]arene and its 'uptake' of non-ionic organic molecules from the aqueous phase

Bengang Xing, Ming-Fai Choi and Bing Xu

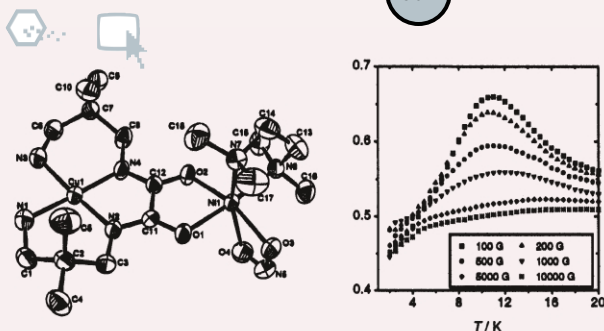


A coordination polymer based, stable organogel ('metalloge'), which 'uptakes' neutral organic molecules from the aqueous phase, may serve as an artificial system to mimic the uptake processes of alkylotrophs.

364

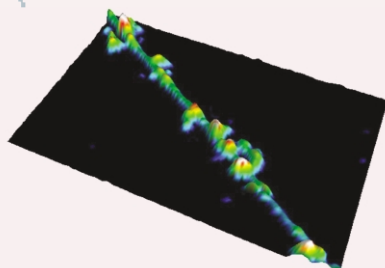
Synthesis and characterization of $[\text{Cu}(\text{Me}_2\text{oxpn})\text{Ni}(\text{NO}_2)\text{-(tmen)}](\text{ClO}_4)_2$: a single ferrimagnetic dinuclear $\text{Cu}^{\text{II}}\text{-Ni}^{\text{II}}$ complex acting as weak molecule-based magnet

Javier Tercero, Carmen Diaz, Joan Ribas, José Mahía and Miguel Maestro



A new heterodinuclear $\text{Ni}^{\text{II}}\text{-Cu}^{\text{II}}$ complex shows ferromagnetic ordering at low temperature. It is one of the very few compounds made from isolated molecules that lead to cooperative magnetic behavior.

366

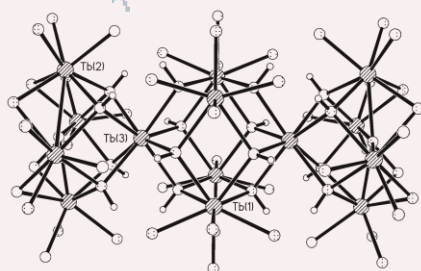


Directly observed covalent coupling of quantum dots to single-wall carbon nanotubes

Bobak R. Azamian, Karl S. Coleman, Jason J. Davis, Neal Hanson and Malcolm L. H. Green

Metal nanoparticles have been covalently coupled to single-walled carbon nanotube termini and side-walls, with the process monitored by atomic force microscopy.

368

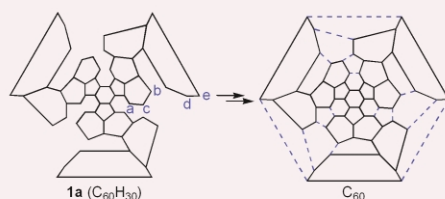


Toward constructing nanoscale hydroxo-lanthanide clusters: syntheses and characterizations of novel tetradecanuclear hydroxo-lanthanide clusters

Ruiyao Wang, Datong Song and Suning Wang

An unprecedented new member of hydroxo-lanthanide cluster compounds, $\text{Ln}_{14}(\mu_4\text{-OH})_2(\mu_3\text{-OH})_{16}(\mu\text{-}\eta^2\text{-acac})_8(\eta^2\text{-acac})_{16}$, that contains a 'hollow' Ln_6 octahedron, has been synthesized and characterized. The core structure of the Ln_{14} ($\text{Ln} = \text{Tb}$) molecule is shown here.

370

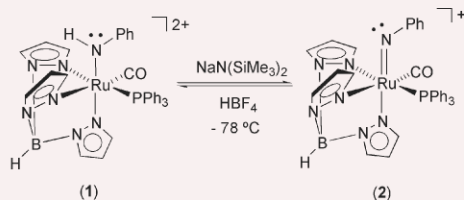


Zippering up 'the crushed fullerene' $\text{C}_{60}\text{H}_{30}$: C_{60} by fifteen-fold, consecutive intramolecular H_2 losses

Berta Gómez-Lor, Carola Koper, Roel H. Fokkens, Edward J. Vlietstra, Thomas J. Cleij, Leonardus W. Jenneskens, Nico M. M. Nibbering and Antonio M. Echavarren

MALDI TOF-MS (positive-ion mode) of tribenzo[*l:l':l''*]benzo[1,2-*e*:3,4-*e'*:5,6-*e''*]triacenanthrylene (**1a**, $\text{C}_{60}\text{H}_{30}$) gives C_{60}^{+} by multiple intramolecular cyclodehydrogenation reactions.

372

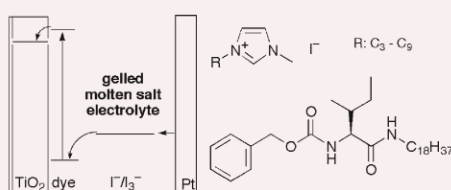


Synthesis of the Ru^{IV} amido complex $[\text{TpRu}(\text{CO})(\text{PPh}_3)(\text{NHP})][\text{OTf}]_2$ (**Tp** = hydridotris(pyrazolyl)borate; **OTf** = trifluoromethanesulfonate) and deprotonation to form an octahedral and d^4 imido complex: computational study of Ru^{IV} -imido bonding

K. N. Jayaprakash, Aaron M. Gillepsie, T. Brent Gunnoe and David P. White

Octahedral and d^4 imido complexes are rarely observed. This report details the generation of the thermally unstable imido complex $[\text{TpRu}(\text{CO})(\text{PPh}_3)(\text{NHP})][\text{OTf}]$ at low temperature along with a computational study of the bonding in the imido complex.

374

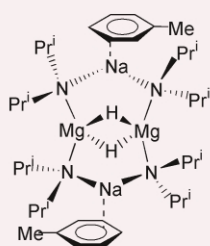


Quasi-solid-state dye-sensitized solar cells using room temperature molten salts and a low molecular weight gelator

Wataru Kubo, Takayuki Kitamura, Kenji Hanabusa, Yuji Wada and Shozo Yanagida

A dye-sensitized solar cell fabricated using imidazolium iodide, iodine and a gelator as a solvent-free quasi-solid-state electrolyte showed a 5.0% conversion efficiency and high-temperature stability.

376

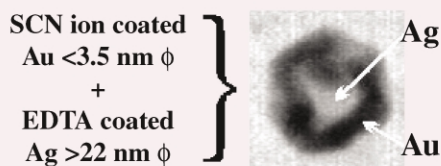


Hydride encapsulation in s-block metal inverse crown chemistry

Daniel J. Gallagher, Kenneth W. Henderson, Alan R. Kennedy, Charles T. O'Hara, Robert E. Mulvey and René B. Rowlings

The first example of hydride encapsulation within a mixed alkali metal–magnesium amide is described, extending yet further the range of so called inverse crown complexes.

378

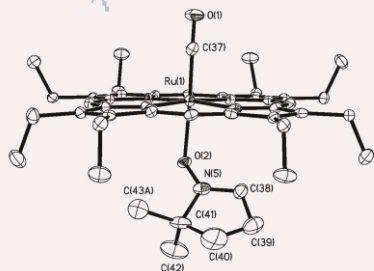


Size quantized formation and self-assembly of gold encased silver nanoparticles

Eliza Hutter and Janos H. Fendler

Mixing aqueous dispersions of thiocyanate ion coated small (<3.5 nm diameter) gold nanoparticles and EDTA covered larger (>22 nm diameter) silver nanoparticles, results in the formation of robust gold encased silver nanoparticles; in contrast to using larger (>11 nm diameter) gold nanoparticles which forms chained structures.

380

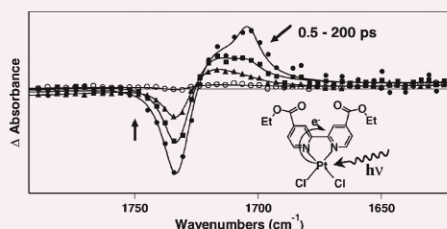


Nitrones are suitable ligands for heme models: X-ray crystal structure of the first metalloporphyrin nitron complex

Jonghyuk Lee, Brendan Twamley and George B. Richter-Addo

Some nitrones are products of heme-dependent metabolism of N-containing compounds. This study shows, for the first time, that nitrones are good ligands for heme models.

382

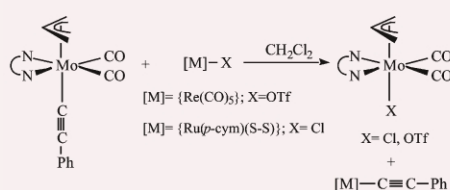


Picosecond time-resolved infrared spectroscopic investigation of excited state dynamics in a Pt^{II} diimine chromophore

Julia A. Weinstein, David C. Grills, Michael Towrie, Pavel Matousek, Anthony W. Parker and Michael W. George

This is the first application of picosecond time-resolved infrared (TRIR) spectroscopy to a d⁸ metal chromophore, Pt(4,4'-(CO₂Et)₂-2,2'-bpy)Cl₂, leading to an MLCT assignment of the lowest excited state with an 8.7 ps lifetime.

384



Molybdenum alkynyls as alkynyl transfer reagents

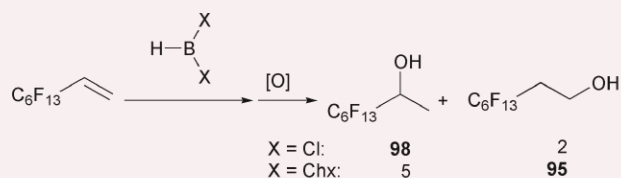
Julio Pérez, Lucía Riera, Víctor Riera, Santiago García-Granda, Esther García-Rodríguez and Daniel Miguel

New alkynyl complexes [Mo(C≡CR)(η^3 -allyl)(CO)₂(phen)], easily prepared and handled, efficiently transfer the alkynyl group to other metal fragments under mild conditions, a property that correlates with their long Mo–C(alkynyl) bond distances.

386

Investigation of the factors controlling the regioselectivity of the hydroboration of fluoroolefins

P. Veeraraghavan Ramachandran and Michael P. Jennings

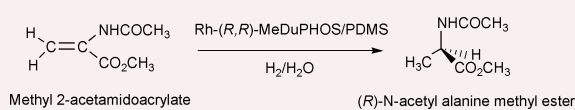


Either Markovnikov or anti-Markovnikov regioselectivity can be achieved at will during the hydroboration–oxidation of perfluoroalkyl(aryl)ethylenes by varying the hydroborating agent.

388

Aqueous enantioselective hydrogenation of methyl 2-acetamidoacrylate with Rh–MeDuPHOS occluded in PDMS

Adi Wolfson, Sofie Janssens, Ivo Vankelecom, Shimona Geresh, Moshe Gottlieb and Moti Herskowitz

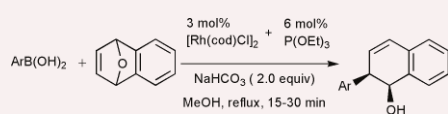


Asymmetric hydrogenation of methyl 2-acetamidoacrylate was performed in water with occluded Rh–MeDuPHOS in a PDMS polymer film. Due to low leaching of catalyst into water and the lack of solubility in the aqueous medium, the recyclable system represents an excellent example of ‘green’ chemistry.

390

Rhodium-catalysed addition of arylboronic acids to oxabenzonorbornadienes

Masahiro Murakami and Hideyuki Igawa



A rhodium(I) complex having P(OEt)_3 ligands catalyses the addition reaction of boronic acids to oxabenzonorbornadienes, affording *cis*-2-aryl-1,2-dihydro-1-naphthol stereoselectively, and in good yield without concomitant deboronation of the boronic acid.

ADDITIONS AND CORRECTIONS

392

Haoguo Zhu, Deborah J. Jones, Jerzy Zajac, Jacques Rozière and Roger Dutartre

Periodic large mesoporous organosilicas from lyotropic liquid crystal polymer templates

CONFERENCE DIARY

xii

COPIES OF CITED ARTICLES

The Library and Information Centre (LIC) of the RSC offers a first class Document Delivery Service for items in Chemistry and related subjects. Contact the LIC, The Royal Society of Chemistry, Burlington House, Piccadilly, London W1V 0BN, UK.

This service is only available from the LIC in London and not the RSC in Cambridge.

Contents lists in advance of publication are available on the web via www.rsc.org/chemcomm – or take advantage of our free e-mail alerting service (www.rsc.org/ej_alert) to receive notification each time a new list becomes available.



Supplementary crystallographic data are available: see article for further information.



Electronic supplementary information is available on <http://www.rsc.org/esi>: see article for further information.

- Abouderbala, Lagili O., 358
 Amorós, Pedro, 330
 Azamian, Bobak R., 366
 Belcher, Warwick J., 358
 Beltrán, Aurelio, 330
 Beltrán, Daniel, 330
 Black, Daniel, 340
 Blake, Alexander J., 340
 Boschetti, Frédéric, 312
 Boutelle, Martyn G., 358
 Brown, John M., 308, 310
 Bucher, Christophe, 328
 Caldés, Maite, 330
 Campbell, Tom, 304
 Carrell, H. L., 344
 Carty, Arthur J., 320
 Cesario, Michele, 326
 Choi, Ming-Fai, 362
 Clarke, Adam J., 352
 Cleij, Thomas J., 370
 Coleman, Anthony W., 326
 Coleman, Karl S., 366
 Corma, Avelino, 334
 Cragg, Peter J., 358
 Crossley, Maxwell J., 356
 Davies, Brian, 332
 Davis, Jason J., 366
 de Keijzer, Adrianus H. J. F., 348
 de Zárate, David Ortiz, 330
 Deerenberg, Sirik, 348
 Dembinski, Roman, 332
 Denat, Franck, 312
 Dent, Andrew J., 304
 Descalzo, Ana B., 330
 Desiraju, Gautam R., 344
 Dhaliwal, Jaspreet, 358
 Diaz, Carmen, 364
 Diaz-Moreno, Sofia, 304
 Dong, A. G., 350
 Dunford, Adrian J., 360
 Dutarte, Roger, 392
 E, Wenbo, 356
 Echavarren, Antonio M., 370
 El Haskouri, Jamal, 330
 Esho, Noor, 332
 Espinosa, Enrique, 312
 Evans, John, 304
 Fabre, Muriel, 358
 Farrington, Edward J., 308
 Fendler, Janos H., 378
 Fiddy, Steven G., 304
 Field, Jason E., 306
 Finn, Rachel L., 340
 Fokkens, Roel H., 370
 Fornés, Vicente, 334
 Fukuzumi, Shunichi, 356
 Gallagher, Daniel J., 376
 Galletero, María S., 334
 Gao, Z., 350
 García, Hermenegildo, 334
 García-Granda, Santiago, 384
 García-Rodríguez, Esther, 384
 George, Michael W., 382
 Geresh, Shimona, 388
 Gillepsie, Aaron M., 372
 Gómez-Lor, Berta, 370
 Goreloff, Philippe, 326
 Gottlieb, Moshe, 388
 Green, Malcolm L. H., 366
 Grills, David C., 382
 Guilard, Roger, 312
 Guillem, Carmen, 330
 Gunnoe, T. Brent, 372
 Hanabusa, Kenji, 374
 Hanson, Neal, 366
 Harada, Yukako, 324
 Henderson, Kenneth W., 376
 Henderson, Richard A., 360
 Herskowitz, Moti, 388
 Holden, Marcia J., 318
 Hoshino, Tsutomu, 291
 Hutter, Eliza, 378
 Igawa, Hideyuki, 390
 Ioannou, Maria, 346
 Jackson, Richard A., 352
 Janssens, Sofie, 388
 Jayaprakash, K. N., 372
 Jenneskens, Leonardus W., 370
 Jennings, Michael C., 354
 Jennings, Michael P., 386
 Jones, Deborah J., 392
 Kadish, Karl M., 356
 Katz, Amy K., 344
 Kawase, Takeshi, 324
 Kennedy, Alan R., 376
 Kimberley, Brian S., 352
 Kitamura, Takayuki, 374
 Knight, Paul D., 352
 Koper, Carola, 370
 Kranenburg, Mirko, 348
 Kubo, Wataru, 374
 Kunwar, A. C., 314
 Lammertsma, Koop, 348
 Latorre, Julio, 330
 Lee, Janet, 332
 Lee, Jonghyuk, 380
 Lindoy, Leonard F., 340
 Lutz, Martin, 348
 Lynch, Vincent, 328
 Maas, Gerhard, 338
 Maeda, Kenji, 310
 Maeda, Shin-ichiro, 316
 Maestro, Miguel, 364
 Mahía, José, 364
 Marcos, M. Dolores, 330
 Martínez-Máñez, Ramón, 330
 Matousek, Pavel, 382
 Matsumoto, Kouzou, 324
 Mayhew, Martin P., 318
 Miguel, Daniel, 384
 Mulvey, Robert E., 376
 Murakami, Masahiro, 390
 Muraleedharan, K. M., 314
 Namboodiri, Vasudevan V., 342
 Newton, Mark A., 304
 Nezhadali, Azizollah, 340
 Nibbering, Nico M. M., 370
 Oda, Masaji, 324
 O'Hara, Charles T., 376
 Ohkubo, Kei, 356
 Ohno, Hiroaki, 316
 Oku, Takeo, 302
 Okumura, Mitsuaki, 316
 Ou, Zhongping, 356
 Parker, Anthony W., 382
 Pérez, Julio, 384
 Porter, Michael J., 346
 Puddephatt, Richard J., 354
 Pyykkö, Pekka, 336
 Qin, Zengquan, 354
 Ramachandran, P.
 Veeraraghavan, 386
 Ranganathan, S., 314
 Reipa, Vytas, 318
 Ren, N., 350
 Ribas, Joan, 364
 Richter-Addo, George B., 380
 Riera, Lucía, 384
 Riera, Víctor, 384
 Rodríguez-López, Gertrudis,
 330
 Rougnaghi, Gholamhossein,
 340
 Rowlings, René B., 376
 Rozière, Jacques, 392
 Saez, Fabienne, 346
 Sankar, A. Ravi, 314
 Sato, Tsutomu, 291
 Scaiano, J. C., 334
 Schakel, Marius, 348
 Schröder, Martin, 340
 Scoles, Ludmila, 320
 Scott, Peter, 352
 Seidel, Daniel, 328
 Seitz, Jürgen, 338
 Sessler, Jonathan L., 328
 Shahgaldian, Patrick, 326
 Shao, Jianguo, 356
 Santic, Paul J., 356
 Song, Datong, 368
 Spek, Anthony L., 348
 Steed, Jonathan W., 358
 Steel, Peter J., 322
 Stenberg, Brian T., 320
 Sumbly, Christopher J., 322
 Tamm, Toomas, 336
 Tanaka, Tetsuaki, 316
 Tang, Y., 350
 Tasker, Peter A., 340
 Tercero, Javier, 364
 Thallapally, Praveen K., 344
 Towrie, Michael, 382
 Turin, Sandra, 304
 Turner, David R., 358
 Twamley, Brendan, 380
 Udachin, Konstantin A., 320
 Vairamani, M., 314
 van Koten, Gerard, 308
 Vankelecom, Ivo, 388
 Varma, Rajender S., 342
 Venkataraman, D., 306
 Vilker, Vincent L., 318
 Viviente, Eloisa Martinez, 308
 Vlietstra, Edward J., 370
 Wada, Yuji, 374
 Wakayama, Ryutaro, 316
 Wallace, Karl J., 358
 Wang, Ruiyao, 368
 Wang, Suning, 368
 Wang, Y. J., 350
 Weinstein, Julia A., 382
 White, David P., 372
 Williams, B. Scott, 308
 Wolfson, Adi, 388
 Xing, Bengang, 362
 Xu, Bing, 362
 Yanagida, Shozo, 374
 Yang, W. L., 350
 Zajac, Jerzy, 392
 Zhu, Haoguo, 392